ОБЪЕДИНЕННЫЙ
ИНСТИТУТ
ЯДЕРНЫХ
ИССЛЕДОВАНИЙ

Дубна

E13-96-179

V.V.Nietz

USE OF PULSED MAGNETIC FIELDS IN NEUTRON SCATTERING STUDIES OF CRYSTALS

Submitted to «Journal of Neutron Research»

1996

1. Introduction

At almost all magnetic laboratories, a pulsed magnetic field on the order of 10^5 *Oe* is used in investigations of the magnetic properties of condensed matter. This is explained by two facts: first, to obtain a constant magnetic field exceeding *80 - 100 kOe* is difficult in practice; second, even such a moderate field as $(1\text{-}3)\cdot 10^5$ *Oe* enables the study of a broad range of physical problems connected with the change in states of magnetically ordered substances. At the same time, the physicists dealing with neutron research make use of pulsed magnetic fields rather rarely, despite having sufficiently powerful neutron sources at hand. Apparently, neutron physicists believe that to obtain a magnetic field exceeding *100 - 150 kOe* is a complex technical task. For instance, one of the available facilities carrying out neutron investigations in a pulsed magnetic field is called a "Diffractometer under Extreme Conditions". For the physicist expert in magnetism, however, a field of several hundred *kOe* is not extreme, by far. Of course, for neutron research one needs to operate a pulsed magnetic facility more powerful and more complex than the ordinary instruments at universities. There, for measurements by "classical" techniques (magnetization, magnetistriction effects, magnetic susceptibility, magnetocalorimetric effects or for Mossbauer effect studies) even single pulses of a field are sufficient. In neutron research, it is necessary to achieve multiple and stable long-term repetitions of pulses in order to obtain sufficient statistics. But experience has shown that such a pulsed field facility is hardly more complex than many of the contemporary neutron spectrometers in use for condensed matter research.

This paper can not be regarded as a review of existing neutron instruments using pulsed magnetic fields, because there are only two such spectrometers of periodic action worldwide. At most, it is an attempt to review the existing but almost unutilized possibilities to implement the pulsed field technique at neutron sources, both steady-state and pulsed. We restrict ourselves here mainly to analysis of the peculiarities of methodology that should be taken into consideration when using a pulsed field in neutron investigations of condensed matter with different sources.

2. Time and magnetic field resolution

It is usually believed that when using pulsed neutron sources, the time resolution and the resolution of the magnitude of the magnetic field applied to the sample associated with it, are totally determined by the duration of the neutron burst. Actually, for a rapid change in the sample state, these resolutions are determined only by the degree of mixing of the sample information during its transfer from the sample to the recording system. In the cases considered below, this transfer is made by neutrons of wavelength λ spread over the limited range $\Delta\lambda$. If the distance between the sample and the detector is denoted by L_2 then the time resolution $\Delta t = c \times L_2 \times \Delta\lambda$, where $c = 2.52\ \mu s \text{Å}^{-1} cm^{-1}$. The quantity $\Delta\lambda$ is determined by the collimation of the neutron beam, the mosaicity of the single crystal (monochromator or sample) or the wavelength range of the neutrons passing through the

sample at a given moment of time. As a result, one obtains the following expression for the time resolution [1]:

$$\Delta t = c\sqrt{(L_2\Delta\lambda)^2 + (\lambda_0\Delta L_2)^2}, \quad (1)$$

where

$$\Delta\lambda = \left[\left(\frac{cL_1}{\tau_s}\right)^2 + \left(\frac{tg\theta_0}{\lambda_0\Delta\theta}\right)^2\right]^{-0.5}, \quad (2)$$

L_1 is the distance between the neutron source and the sample, τ_s is the duration of the source burst (in μs), $\Delta\theta$ is the uncertainty in the value of the Bragg angle related to the sample mosaic structure and beam collimation, and ΔL_2 is the uncertainty in the flight distance related to sample size and detector thickness. In correspondence with (1), (2), it is possible to reach a time resolution equal to *2-4* μs. These relations are true for a steady-state reactor ($\tau_s \to \infty$), as well.

For sinusoidal pulses of a field with an amplitude H_m and a duration (half-period of the sine wave) T_H, the relative field resolution is:

$$\frac{\Delta H}{H_m} = \frac{\pi}{T_H}\cdot\Delta t\cdot\left|\cos\pi\frac{t}{T_H}\right|. \quad (3)$$

It is totally unjustified, when measuring the field dependence of the elastic neutron scattering intensity with a pulsed neutron source, to make an effort to increase the magnetic field duration or to get a flat pulse top in order to consider the field magnitude as constant within the diffraction peak profile. The main limitation to the pulse repetition is connected with heating of the magnet. In experiments with diffraction on single crystals, information on the magnetic state is in only one, two or three, but not more, peaks which are separated by large time intervals and consequently can not be penetrated by one magnetic pulse.

Thus, one ought to set the duration of the pulses as near to the diffraction peak duration as possible. Use of magnetic field pulses with a duration which is comparative to the diffraction peak widths, permits the frequency of these pulses to be increased and by that, to decrease the time necessary to obtain the diffraction results. Usually, it is necessary in an experiment to get the dependence of the scattering intensity on the field value, starting from small magnitudes. In the case of short magnetic pulses, one obtains the scattering ability of the sample, as a function of the field value, simultaneously.

3. Linear dependence of intensity on the effective structure factor

When using a pulsed magnetic field one has to get as high a neutron scattering intensity as possible. If the dependence of the orientation of the magnetic sublattices on field magnitude is to be determined, one has to ensure the fulfillment of conditions where the relationship between the intensity and the effective structure factor is considered unambiguously and is well known in advance. But, the conditions for applying the kinematic approximation, where intensity is proportional to the square of the structure factor, are not the optimum ones.

A substantially higher intensity can be ensured by making use of relatively thick samples. If a crystal consists of sufficiently large crystallites, then in a certain range of structure factor values, the diffraction scattering intensity is proportional to the structure factor [2]. Figure 1 shows the dependence $I(F)$ which illustrates this case. In the interval from F_1 to F_2 the diffraction on each crystallite obeys the dynamic theory, but the scattering functions of different crystallites do not overlap. In other words, the overall intensity is simply a sum of the reflected intensities from all crystallites of the sample. For higher F values, the linear dependence is broken due to the overlap in the scattering functions of individual microcrystallites, i.e., due to secondary extinction. For very small values of F in the "thick sample" case, we get a quadratic dependence.

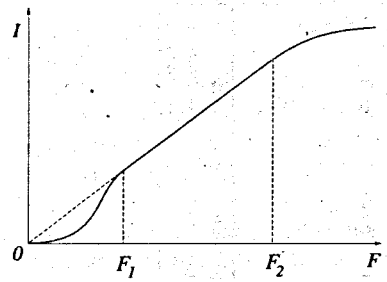

Fig.1 The dependence of diffraction intensity on the structure factor F for a single crystal consisting of large crystallites. At the condition $F_1 < F < F_2$ the dependence is close to linear.

By properly selecting the Bragg angle and crystal thickness, one can locate the corresponding range (F_1F_2) where a change in F under the action of a magnetic field can be expected. Our experience has shown that for the majority of single crystals prepared by ordinary techniques, the "large crystallites" condition can be satisfied for diffraction reflections of moderate intensity, i.e., using samples with a thickness of several millimeters permits a sufficiently broad range of linearity. Measurements with such crystals require a preliminary empirical selection of the operating conditions appropriate to the specific physical task. Useful for the purpose is the presence of different known phase states of the substance which can be initiated by changing the temperature or applying a weak magnetic field. In turn, we get rid of the rather laborious and essentially useless procedure of determining such crystal parameters as mosaicity and crystallite sizes. The intensity of diffraction reflections corresponding to the linear dependence range can, in some cases, be an order of magnitude or higher compared to thin crystals and the kinematic approximation.

4. Diffraction with a pulsed magnetic field at pulsed neutron sources

The comparative characteristics of the different neutron sources that can be used for condensed matter research with a pulsed field are presented in the Table. Here P_1 is the flux density of neutrons falling on the sample per field pulse; $\Delta\lambda_m = \lambda_0\eta / tg\theta_0$ is the wavelength range connected with the mosaicity η of the crystal sample at $\theta_0 = 45°$, $\eta = 5'$. Thus, the value $P_1\Delta\lambda_m$ equals the quantity of neutrons scattered per field pulse at full reflectivity from a crystal.

Table. Comparison of the intensities at an operation with a pulsed magnetic field on different neutron sources

	units	IBR-2, SNIM-2	ISIS	KEK	SPTR	SPR-III	HFR,ILL(*57MW*)	ESS(project)
Peak density flux, P	$ncm^{-2}s^{-1}$	$7 \cdot 10^{15}$	$1.4 \cdot 10^{15}$		10^{16}-10^{18}	10^{18}	$1.5 \cdot 10^{15}$	$4 \cdot 10^{16}$
Pulse duration, τ_i	μs	300	70	150	10^3-10^5	75		70
Frequency,	sec^{-1}	5	50	20	$\equiv$ *1 pulse/hour*			50
Average flux of thermal neutrons at the sample position	$ncm^{-2}s^{-1}$	$4 \cdot 10^6$ (water moder.)	$4 \cdot 10^7$ (IRIS, hydr. moder.) $4.5 \cdot 10^6$ (meth.moder.)	$5 \cdot 10^5$			10^9	10^9
$P_1(3Å)$	$ncm^{-2}Å^{-1}pulse^{-1}$	$2.5 \cdot 10^5$ (water moder.) $1 \cdot 10^6$ (meth. moder.)	$0.9 \cdot 10^5$ (hydr. moder.)	$2.8 \cdot 10^3$ (hydr.moder)	10^7-10^9 (for *10 ms*)	$3.2 \cdot 10^5$ (for *10 μs*)	$3 \cdot 10^6$ (for *5 ms*)	$2.6 \cdot 10^6$ (hydr. moder.)
$P_1(2Å)$		$4 \cdot 10^5$ (water moder.)	$0.35 \cdot 10^5$ (meth. moder)					
$P_1 \Delta\lambda_m$ (3Å)	$ncm^{-2}pulse^{-1}$	$1 \cdot 10^3$ (water moder.)	$0.37 \cdot 10^3$ (hydr. moder.)	10	$(0.4\text{-}40) \cdot 10^5$ (for *10 ms*)	10^4 (for *10 μs* at L_1 = *500 cm*)	$1.2 \cdot 10^4$ (for *5 ms*)	$1 \cdot 10^4$ (hydr. moder.)

a) Pulsing reactors

Diffraction investigations in a pulsed magnetic field on the pulsing reactors of JINR-Dubna (IBR, IBR-30 and IBR-2) have been carried out since 1968 [3-16]. The present-day pulsed magnetic facility, SNIM-2, operating at IBR-2 (*2 MW*) is described in refs. [17,18]. The duration of the magnetic pulses on this spectrometer, with the magnets now in use, can be changed within limits from *500* to *2000 μs*. (The magnetic facility permits pulses with a duration up to *5 - 10 ms* if magnets with a larger inductance are used.) The amplitude of the pulses are now up to *200 kOe*. However, the real possibilities of magnetic facility are limited only by the magnets, at present. The current amplitude for *200 kOe* is about *50 kA*, but the SNIM-2 permits current pulses up to *120 - 150 kA* to be obtained. The minimum temperature for measurements with a magnetic field on SNIM-2 is only *35 K*, at present.

It is necessary to note that the optimum time duration of the thermal neutron flush for diffraction measurements is *1 - 3 ms*. This is determined by the typical duration of the magnetic pulses with the use of standard electrical equipment. Besides, at a magnetic pulse time duration of less than *500 μs*, the real field resolution deteriorates, in accordance with (3).

SNIM-2 is suitable for the study of not only the structure of field induced quasi-stationary phase states, but also the kinetics of phase changes in single crystals. The stability of the facility operation and accuracy of the measurements allow reliable identification of hysteresis loops at first order phase transitions with a relative width of *0.5%* [19]. The most recent experiment on SNIM-2 was the observation of the weak antiferromagnetism induced by an external field in the rare earth orthoferrite $HoFeO_3$ and determination of the "antiferromagnetic susceptibility" associated with the rare earth ions [20]. This investigation permitted the very small, *0.05* μ_B per ion, component of induced antiferromagnetic ordering to be registered which has not been achieved by other methods.

b) Single pulsed thermal reactors (SPTR)

There are interesting possibilities for using pulsed fields on pulsed thermal reactors which are operated in the regime of single power pulses. At their peak power, they produce neutron fluxes up to 10^{17}-10^{18} *n/(cm²s)*, which are two to three orders of magnitude higher than the steady fluxes produced by the most advanced research reactors. The time width of these pulses in the single burst regime is most commonly in the range *5 - 50 ms*, with the narrowest pulse width being about *2 ms*. The most numerous family of such neutron sources are the pulse reactors which are cooled and moderated by light water. These are the TRIGA, SPERT, PULSTAR, KEWB, IIN reactors and others [21-26]. Near *40* TRIGA reactors have been built and about of half of them have a pulsing mechanism built into them. There are several homogeneous graphite reactors, TREAT, FLESH, IGR and BIGR [21,23,27,28,29]. The peak neutron flux for BIGR is about 10^{18} *therm.n/(cm²s)* at the duration of the pulse about *2 ms*.

The diffractometer with a high pulsed magnetic field is used in condensed matter research on the TRIGA-reactor of Technical University, Vienna, Austria [30,31]. The

reactor operates at a power of about *250 kW* in a steady state regime, but permits single (approximately once per hour) bursts of power up to *400 MW* at a duration up to *30 ms*. This magnetic facility is of non-periodic action. The change in the diffraction intensity for a single MnF_2 crystal under a single magnetic pulse is presented in ref.[31]. The intensity was equal to only *30 - 40* neutrons per pulse in each time channel with the width of *1 ms*. The single crystal samples with a pulsed magnet are disposed on this instrument in the monochromatic neutron beam. This does not allow a sufficiently high intensity of diffraction scattering on the sample. If the crystal were disposed in the "white" neutron beam, it would permit an increase in intensity of one or two orders of magnitude.

It follows from the Table that on SPTRs, at full reflection from a single crystal with a mosaicity of *5'* and an area of *1* cm^2, it is possible to get $(0.4\text{-}4)\cdot 10^5$ scattered neutrons with a wavelength of *3 Å* per magnetic pulse with a duration of *10 ms*. At a duration of one time channel equal to *30 μsec*, this means a count of *100 - 1000* neutrons per channel. In such a case, the relative field resolution (in accordance with (3)) is $\Delta H/H_m \lesssim 0.01$. Optimization of sample sizes, to have a linear dependence between the intensity and the structure factor can produce a good neutron spectrum with several tens of pulses of the reactor and magnetic facility. The low frequency of the SPTR is compensated for by higher peak flux and longer burst duration. The necessary information can be obtained with fewer magnetic field pulses than on the IBR-2 reactor.

Practically, because of the terminal strength of magnets, higher reactor power in the single burst regime means, under the same conditions, the possibility of making physical measurements at higher values of the magnetic field than with other neutron sources. If the duration of a burst is equal to a several ten milliseconds, as on the Vienna TRIGA, there is a possibility of measuring the diffraction simultaneously from several crystallographic planes. The essential advantage of such reactors, in comparison with the steady state reactors and neutron sources of periodic action, is the considerable simplification of the problems connected with magnet and sample cooling. Therefore, SPTRs in the single burst regime are the most suitable neutron sources for use with a pulsed magnetic field of *300 - 800 kOe*. In such a case the magnet can be used without destroying it, but it is necessary to allow enough time for it cool it after each pulse (see, for instance, refs.[32,33]).

Use of a pulsed magnetic field on the SPTR is more appropriate for determining the structure of quasi-stationary states where, because of long relaxation times, field pulses with rather long durations (*5 - 10 ms*) are necessary.

c) Spallation sources

Research with pulsed magnetic fields was developed since 1989 at the KENS pulsed spallation neutron source of the National Laboratory for High Energy Physics (KEK, Japan) [34-39]. The device operates on a MRP beamline (Medium Resolution Diffractometer under Extreme Conditions). The diffraction studies of the phase transitions in $PrCo_2Si_2$ and $CsCuCl_3$ with magnetic field pulses with an amplitude up to *140 kOe* were made.

The neutron intensity relating for each pulse of the magnetic field of this facility is at least on two order less than at SNIM-2. It is necessary to note that the IBR-2 reactor ($2MW$, $5\ s^{-1}$) has an advantage over pulsed neutron spallation sources due to its low power

pulse repetition and correspondingly larger instantaneous flux of thermal neutrons. Because of the limited magnetic pulse frequency and relatively high repetition frequency of the spallation source, it is possible to use only a small number of the neutron bursts (according to [35], only 1/40). The maximum energy stored on the MRP diffractometer is *50 kJ*, in comparison with *300 kJ* on SNIM-2. The operating conditions with thermal neutrons for condensed matter research at KEK-NS are comparable to the conditions which were at IBR-30 ($24\ kW$, $5\ s^{-1}$).

There are good perspectives for investigations with a pulsed magnetic field on the ISIS spallation source [40]. The average flux of thermal neutrons [41] at the possible sample position using a liquid hydrogen moderator is more than one order of magnitude greater than those now on SNIM-2 with a water moderator. But, because of the higher repetition frequency in comparison with IBR-2, the count P_1 of neutrons which can be used per pulse, for instance at a wavelength of *3 Å*, is less than on SNIM-2 (see Table).

The data for MRP-KEK in the Table are shown, assuming the use of a liquid hydrogen moderator as at the ISIS source.

For comparison, estimations of the intensity for one of the projected accelerator based neutron sources, the European Spallation Source [42], are presented in the eighth column of the Table, as well. The average thermal neutron flux and other data were deduced by analogy from conditions at ISIS (the use of neutron guides and a liquid hydrogen moderator).

d) Research with a single pulse of an ultra-strong magnetic field

An "ultra-strong" magnetic field is a field of several *MOe*. In practice, such a field can be obtained only in the form of very short single pulses, when the magnet and its contents are destroyed. A field with an amplitude of up to $(1\text{-}3)\cdot 10^6$ *Oe* can be generated by a several *MA* pulse of current flowing through a magnet (as a rule, a single coil is used in such case). In order to reach higher field magnitudes, a preliminary pulse with an amplitude of about $(1\text{-}2)\cdot 10^5$ *Oe* with a duration of several hundred microseconds is generated in a multiple coil magnet, and then, when the field value is near its maximum magnitude, the magnetic flux is compressed by electromagnetic methods or by exploding the blasting charge which surrounds the magnet. Field pulses with amplitudes up to $(3\text{-}10)\cdot 10^6$ *Oe* can been obtained by this method at a pulse duration of *5-10 μs* [43-59]. To use such magnetic fields, it is necessary to have a time resolution of about *1-2 μs* and a neutron intensity in the primary beam sufficient to measure the field dependence of the scattering with only one pulse of the field.

With the exception of nuclear explosions, the most intense pulse fluxes of neutrons are in the "fast burst reactors", i.e., reactors with fast neutrons generating short power pulses due to self-extinction of the fission. An alloy of ^{235}U and 1.5-10% Mo is used as the fuel in these reactors: HPRR, Super Kukla, Godiva IV, SPR II, SPR III, APRFR and Caliban [60-63]. For instance, the peak density of neutron flux in the core of the Sandia Pulse Reactor, SPR-III [63], is equal to $7.4\cdot 10^{18} n/(cm^2 s)$ at a pulse width of *75 μs*.

It is necessary to note that with diffraction on a single crystal in a magnetic field, there are serious restrictions on the choice of scattering angle. These restrictions are especially limiting with the use of ultra-strong fields where registration of the scattered beam is

possible only at an angle near 0° or 180° relative to the primary beam. Measurements by neutron transmission through a single crystal may be preferable (see Fig.2) in such cases [64]. The magnet, with the sample and the detector, are set in the "white" beam of a pulse reactor and the downfall in the spectrum, due to diffraction on the chosen crystallographic plane, is measured (see Fig.3).

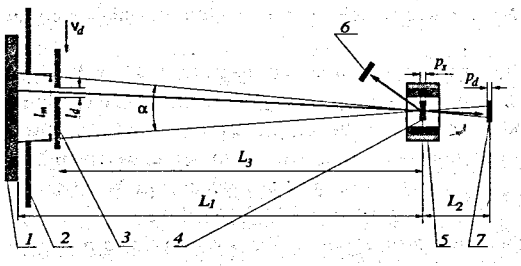

Fig.2 Disposition of equipment for a diffraction measurement using a pulsed neutron source with transmission of the neutrons through a single crystal: 1 - moderator; 2 - diaphragm, limiting the angle diapason of the neutrons falling on the sample; 4 - single crystal; 5 - magnet , with a horisontal field; 6 - detector registering the beam of diffracted neutrons; 7 - detector registering the neutrons passing through the sample; 8 - moving slit diaphragm.

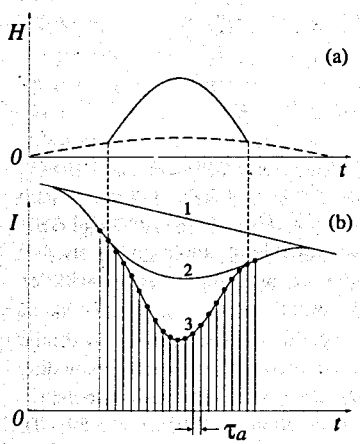

Fig.3 Measurement of the field dependence of diffraction scattering from a preset crystallographic plane: a) dependence of field value on time; b) time dependence for the intensity of the neutrons passing through a single crystal: 1 - intensity without sample, 2 - with sample without magnetic field, 3 - intensity at the change of the reflection possibility of a single crystal under the action of a magnetic field; τ_a - time analizer channel width.

Let us introduce the following notations: $\Delta\lambda_1 = \frac{\tau_s}{cL_1}$ is the degree of instantaneous monochromaticity of the primary beam; $\Delta\lambda_2 = \lambda_0\eta / tg\theta_0$ is the wavelength range of neutrons scattered on the sample at a fixed angle of incidence, where η is the mosaicity of the crystal; $\Delta\lambda_3 = \lambda_0\alpha / tg\theta_0$ is the wavelength range related to the angular divergence α of the incident neutron beam. In order to decrease the background contribution of neutrons which are produced from the moderator sides and do not satisfy the Bragg condition, it is advisable to limit the width of the visible portion of the moderator to the value l_m determined by the condition $\Delta\lambda_1 = \Delta\lambda_3$.

Let $P_{th}(\lambda)\Delta\lambda$ be the quantity of thermal neutrons in the interval $\Delta\lambda$ which are emitted from *1* cm^2 of moderator surface per *second*. By approximating the time shape of the reactor power burst with a rectangular function of width τ_s and by taking into account that the wavelength range $\Delta\lambda$ of neutrons incident on the sample at any moment of time is $\Delta\lambda_1$, for the number of neutrons incident on the sample per *second* we get:

$$I_0 = \frac{h\,s\,\tau_s^2\,tg\theta_0}{2\pi\,c^2\lambda_0 L_1^3} P_{th}(\lambda_0), \tag{4}$$

where h is the height of the visible part of the moderator and s is the area of the sample.

The probability of neutron scattering, and hence, the depth of the downfall within the transmitted spectrum, can be characterized by the product of two coefficients. The first - k - is the probability that an incident neutron satisfies the Bragg condition, i.e., is in the interval $\Delta\lambda_2$; consequently,

$$k = \begin{cases} \dfrac{c\,\lambda_0\,\eta\,L_1}{\tau_s\,tg\theta_0}, & \text{if } \Delta\lambda_2 < \Delta\lambda_1, \\ 1, & \text{if } \Delta\lambda_2 > \Delta\lambda_1. \end{cases} \tag{5}$$

The second coefficient - K - is the probability of scattering for a neutron satisfying the Bragg condition. This coefficient is a characteristic of the scattering ability of the sample. It is determined by the correlation between the sample thickness, its mosaicity, the structure factor, and the magnitude of the magnetic moments, and is dependent on the external field magnitude. In the case of scattering saturation, the coefficient $K \cong 1$ (neglecting absorption, and incoherent and inelastic scattering, as well). For the scattering intensity to be sufficiently dependent on the magnetic field, it is expedient to make K substantially different from *1*, for instance *0.3 - 0.5*, which is usually easy to ensure by selecting an appropriate sample thickness. Thus, the scattering intensity is $I_s = kKI_0$.

Usually, the SPR-type reactors do not have neutron moderators and channels for selecting thermal neutrons. Of course, these installations would considerably decrease the effective neutron flux. So, for the estimation of the intensity, we have taken the peak flux value of fast neutrons as only $P = 1\cdot10^{18}$ *n/(cm²s)* (see Table).

Let $\int P_{th}(\lambda)d\lambda$ be equal to *0.15P*, assuming that only *15%* of the fast neutrons become thermal as a result of moderation. Assuming that the thermal spectrum width is equal to *4 Å*, for $\lambda_0 = 3$ *Å* and $P = 10^{18}$ *n/(cm²s)*: $P_{th}(3Å) = 10^{16}$ *n/(cm²Ås)*. In the case where the distance between the moderator and the sample $L_1 = 500$ *cm*, $s = 1cm^2$, $h = 10$ *cm*, $\theta_0 = 45°$, $\eta = 5'$, $\tau_s = 70$ *μs* and $K = 0.5$, one obtains $k = 0.075$, $I_0 = 6.7\cdot10^4$ *n/(2μs)*, $I_s = 2500$ *n/(2μs)*, i.e., when using the reflection geometry, the relative statistical error for one channel with a width of *2 μs* is equal to *2%*. A similar result can be obtained in the reflection geometry at the SPTR (single pulsed thermal reactors) with the most powerful peak neutron fluxes.

To use transmission geometry in an experiment, it is necessary to increase the flight distance, that is L_1, and to decrease the effective neutron pulse width by using a movable diaphragm. This diaphragm is a vertical slit which crosses the beam in a direction corresponding to a decrease in the scattering angle of the neutrons passing through the slit. The diaphragm velocity is set so that neutrons passing through the slit at different

moments of time fall on the sample simultaneously, i.e. $v_d = tg\theta_0 c^{-1}\lambda_0^{-1}$. This way, in the spectrum of neutrons transmitted through the sample, the "background" of neutrons violating Bragg's law is decreased without changing the magnitude of the "effect". For a slit width which is chosen on the basis of the relation $l_d = \eta L_3$, where L_3 is the distance between the slit and the sample, one gets a coefficient k close to unity.

Having in mind that we measure the difference between two spectra - with the crystal and without it - we get the following relation for the relative statistical error of the measurement of crystal scattering ability for the transmission geometry (at a channel width of 2 μs, per magnetic field pulse):

$$\delta K = \frac{\sqrt{1-K}+(1-K)}{K\sqrt{I_0}}\sqrt{\frac{\tau_s\, tg\theta_0}{c\, L_1\, \eta\, \lambda_0}}. \qquad (6)$$

Here I_0 is the neutron intensity on the sample in the absence of the movable diaphragm.

For the above-given example, but at $L_1 = 10^3 cm$ and using the movable diaphragm at a distance $L_3 = 700\ cm$ ($l_d = 1\ cm$, $v_d = 1.33 \cdot 10^3\ cm/s$), one obtains $\delta K = 1.75\%$ for the transmission geometry.

If the distance between the sample and the detector $L_2 = 30\ cm$, and the sizes of the crystal and the detector are $p_s = 0.2\ cm$, $p_d = 0.1\ cm$, respectively, then for the above examples, the time resolutions are: for the case of registering the scattered beam at $L_1 = 500\ cm$, $\Delta t \cong 3.5\ \mu s$; for the transmission geometry at $L_1 = 1000\ cm$ Δt is less than 2 μs.

Using the beam of SPTR, i.e., a reactor with the burst duration of *1 - 50 ms*, the condition $\Delta\lambda_1 = \Delta\lambda_3$ is not fulfilled. In such case the quantity of neutrons incident on the sample per *second* (without the diaphragm) is equal to

$$I_0 = \frac{h\, s\, \tau_s\, l_m}{2\pi\, c L_1^3} P_{th}(\lambda_0), \qquad (7)$$

where l_m is the width of the visible part of the moderator. For the relative statistical error with the transmission geometry in the measurement of crystal scattering ability we obtain, instead of (6), the following expression (at a channel width of 2 μs, per magnetic field pulse):

$$\delta K = \frac{\sqrt{1-K}+(1-K)}{K} L_1 \sqrt{\frac{2\pi\, tg\theta_0}{P_{th} h\, s\, l\, \eta\, \lambda_0}} \qquad (8)$$

If $P_{th} = 10^{16}\ n/(cm^2 Å s)$, $h = 10\ cm$, $l_m = 20\ cm$, $L_1 = 700\ cm$, $s = 1\ cm^2$, $\theta_0 = 45°$, $\eta = 5'$, $\tau_s = 70\ \mu s$, $K = 0.5$, then in the transmission geometry on SPTR with $P = 10^{18} n/(cm^2 s)$, the values $I_0 \cong 6 \cdot 10^4\ n/(2\mu s)$ and $\delta K \cong 2\%$.

5. Diffraction with a pulsed magnetic field at a steady-state reactor

As it follows from Section 2, diffraction measurements in pulsed magnetic fields are possible on the neutron beams of a steady-state reactor. Such research was performed in 1969 [65]. A relatively low-power pulsed magnetic facility was assembled and transported by a single truck to the WWR-C reactor (*10 MW* thermal power, Branch Establishment of Moscow Institute of Physics and Chemistry in Obninsk, 100 km from Moscow). Only three weeks were allocated for physical measurements. The experimental geometry was the

simplest one possible (see Fig.4): a spherical single crystal of hematite (α-Fe_2O_3) with a diameter of *9 mm* was cooled to liquid nitrogen temperatures, and together with the pulsed

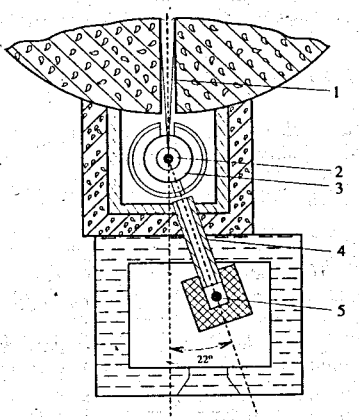

Fig.4 Geometry of a diffraction measurement at a steady-state reactor: 1 - "white" primary beam of neutrons, 2 - the single crystal sample, 3 - the pulsed magnet, 4 - collimator, 5 - detector of scattered neutrons.

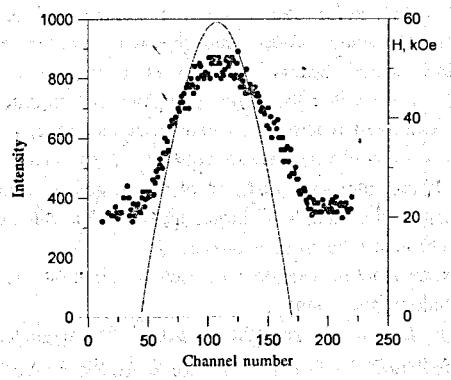

Fig.5 A neutron pattern for the *(111)* reflection obtained with an α-Fe_2O_3 single crystal, which was disposed in the "white" beam of a steady-state reactor. The magnetic field pulses had a half sine shape. Along the horizontal axis are the channel numbers of the time analizer, each channel having a width of *20 μs*.

magnet, was exposed to the "white" beam of the reactor instead of the usual single crystal neutron monochromator. The detector was located *190 cm* from the sample with a scattering angle $2\theta = 22°$ and $\Delta\theta \cong 0.4°$. The magnetic field was vertical. The pulses from the detector were analyzed by a multichannel time analyzer synchronized with the magnetic field pulses.

Fig.5 illustrates a typical neutron diffraction pattern collected with a time analyzer channel width of *20 μs*. Here, the intensity change is connected with the *(111)* reflection, which is absent below the Morin point, and appears due to rotation of the antiferromagnetism vector under the action of the magnetic field perpendicular to the rhombohedral axis of the crystal. The constant background of the neutron spectrum comes from nuclear scattering in the sample and scattering from surrounding objects.

Such neutron patterns as in Fig.5 were obtained with *3000 - 4000* pulses of the magnetic field. One of the physical results of the measurements was the hysteresis in the dependence of scattering intensity on the magnetic field value (upward branch of the hysteresis loop corresponds to the increase in the pulsed field, and the downward, decreasing branch to the decrease in the field). These measurements were not continued because of the low power of the magnetic facility and the primitivness of the pulsed magnet.

One wonders why, in the 25 years since that time, such studies have not been carried out at any of the steady-state reactors, albeit the field range *100 - 300 kOe* is not less useful for studying the magnetic characters of condensed matter than *50 - 100 kOe*, using superconducting magnets.

The estimations for the HRF-reactor (ILL, France, *57 MW*) are presented in the Table, assuming the use of a mirror neutron guide as on the H-22 beamline [66] of this reactor. Here, the intensity I_1 is for *5 ms*. It is possible to generate pulses up to *200 kOe* with a duration of *500 μs* on SNIM-2 in the operating volume about *1 cm*^{3} with a repetition rate of *5 s*$^{-1}$. As the frequency of pulses with a *5 ms* duration can be ten times less than at the duration of *0.5 ms* on SNIM-2, because of induced heating of the magnet, it can be seen that the conditions for obtaining the necessary counts for one diffraction peak at $\lambda = 3Å$ on the HRF-reactor are only three times worse than on SNIM-2-IBR-2 with its methane moderator. Of course, the advantage of using pulse sources is the absence of the "background" connected with reflections of other orders and inelastic scattering. Apparently, diffraction measurements in the "white" beams of steady state reactors are possible for sufficiently intense reflections. A neutron pattern for a sample of hematite, similar to the one used with the WWR-C (Obninsk) reactor, in a magnetic field of *120 - 150 kOe* with a statistical error of *2%* at a time channel width equal to *4 μs*, can be obtained on the HRF reactor in *1-2 hours*. If the interplane distance of the sample is near that of the monochromator, or the mosaicity of the sample is large, the intensity can be sufficient if the sample is placed in a monochromatic beam of neutrons.

The measurement efficiency on steady state reactors can be increased by simultaneous registration of reflections from several crystallographic planes.

For sufficiently large distances between the sample and the detector, the magnetic reflections of different orders become separated in time. For instance, if, in the case of hematite, $L_2 = 200\,cm$, $\theta = 19.1°$ and the magnetic pulse duration $T_H = 1000\,\mu s$, then the magnetic reflections *(111)* and *(333)* are obtained at $\lambda = 3Å$ and $\lambda = 1Å$, respectively, and

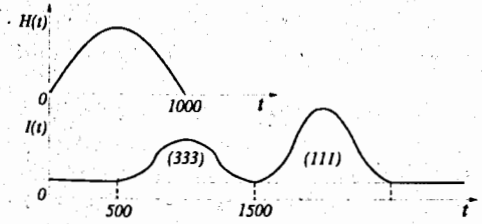

Fig.6 The scheme of separating the *(111)* and *(333)* magnetic reflections for hematite for measurement on a steady-state reactor. The time dependence of the magnetic field is shown at the top, the corresponding neutron time pattern is presented below.

become completely separated (schematically shown in Fig.6). Here, if the collimation of the beam $\Delta\theta = 10'$, then the time resolution Δt is equal to *12.5 μs* for *(111)* and about *4 μs* for *(333)*. Correspondingly, the field resolutions at the pulse start and at the end are equal to *4%* for *(111)* and *1.3%* for *(333)*.

6. Use of a pulsed magnetic field with inelastic neutron scattering

The most obvious task is to measure the change in the dispersion curves under the action of a magnetic field. Figs.7a and 7b illustrate two possible geometries for inelastic coherent scattering measurements using a pulsed magnetic field at a pulsed neutron source.

In the case of preliminary monochromation of the primary neutron beam, by means of a velocity selector or a crystal monochromator, it is possible to measure the intensity of neutrons undergoing inelastic scattering in several crystallographic directions, simultaneously. For this, the wave vector of the incident neutrons has to match, in size and direction, one of the reciprocal lattice vectors (see Fig.7a). Analysis of the energy of the scattered neutrons obviously has to be done by the time-of-flight technique.

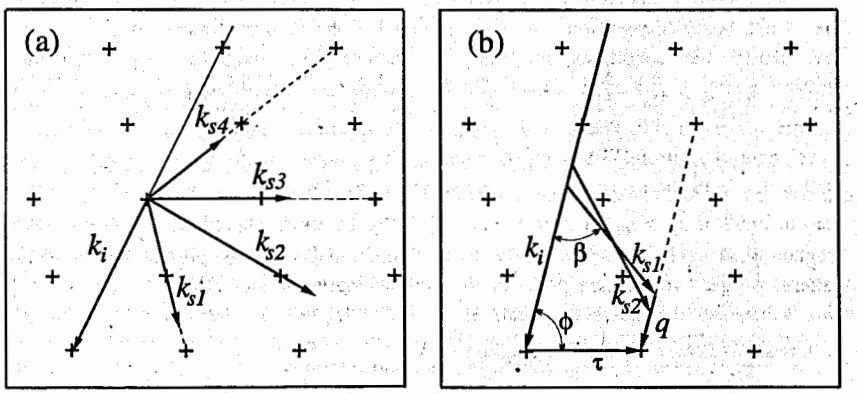

Fig.7 Diagrams of the measurement of dispersion dependencies using a pulsed neutron source and pulsed magnetic field: k_i is the wave vector of falling neutrons; k_{sn} are the wave vectors of scattered neutrons. a) "direct" geometry of the experiment - with the monochromatization of primary neutrons and simultaneous measurement (by the time-of-flight-method) of a neutrons scattered in a few crystallographic directions; b) "inverse" geometry, when the sample is disposed in the "white" primary beam of neutrons and monochromatization of the second beam provides the necessary magnon direction.

In measuring dispersion curves in the inverse geometry [67], the "white" primary neutron beam has to be directed along a preset crystallographic direction of the sample and the scattered neutrons have to be monochromatized according to the condition (see Fig.7b, analogous to operations with the PRISMA spectrometer [68], ISIS):

$$k_s = \tau \frac{\sin\beta}{\sin\varphi}, \qquad (9)$$

where $\tau = |\tau|$ is the magnitude of the reciprocal lattice vector in the vicinity of the measured magnons, β is the scattering angle and φ is the angle between the given crystallographic direction and τ. Fig.8 shows two diagrams corresponding to the change in magnon energy under the action of the applied pulsed magnetic field. The hatched peaks correspond to magnons at $H = 0$, other peaks correspond to magnons under the action of the field. All peaks in Fig.8 are matched with the magnetic field pulse by the corresponding time delay associated with the flight time of scattered neutrons over the distance between the sample and the detector. For the sake of simplicity, we assume that the field pulse has a sine-wave form, i.e., $H = H_m \sin \Omega(t - t_H)$ where t_H is the time delay of the magnetic pulse with respect to the start pulse of the neutron source. Fig.8a illustrates the case when the energy of the primary neutrons, corresponding to scattering on magnons, is reduced by the applied field. For the creation of a magnon, this means that the value of $\omega(k)$ in the magnetic field decreases. And contrariwise, in the case of scattering with magnon annihilation, the quantity $\omega(k)$ in the magnetic field increases. Fig.8b illustrates a counter process, where the incident neutron energy is increased by the applied field. At least, for relatively small magnitudes of the magnetic field, one can suppose that the change in the dispersion curve is proportional to the field magnitude, i.e., the neutrons that satisfy the conditions for inelastic scattering on magnons have wavelengths $\lambda_H(t) = \lambda_0 + a \sin \Omega(t - t_H)$, where λ_0 is the neutron wavelength for a magnon peak in the absence of the field. The straight line in the figure is used to show the change in wavelength of neutrons falling on the sample. New magnon peaks occur at the intersection of this line with the curve $\lambda_H(t)$ as shown in Fig.8a, for $a>0$, and in Fig.8b, for $a<0$. As seen in Fig.8, if $t_H > t_0$ for $a>0$ or $(t_H + T_H) < t_0$ for $a<0$, where t_0 is the location of the magnon peak at $H = 0$, in addition to the initial magnon peak present in the neutron pattern, we get two magnon peaks of the same excitation branch which correspond to the two values of the magnetic field. If $t_H < t_0 < (t_H + T_H)$, the initial magnon peak disappears and there is only one magnon peak.

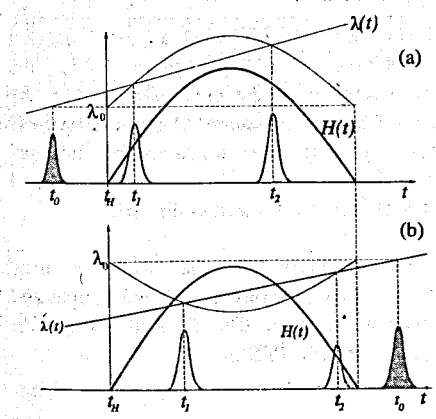

Fig.8 Time relations between the field pulse $H(t)$ and the positions of the magnon peaks with "inverse" geometry: a) the case of a decrease in the primary neutron energy under the action of the field, b) the case of an increase in the primary neutron energy in a magnetic field.

In such an experimental arrangement, the value of the applied field corresponding to the magnon peak is, to some extent, a random quantity and it is necessary to measure the field pulse form precisely. Only for field pulses with a quasi-rectangular shape (with an extended flat top) can the change in $\omega(k)$ be measured by giving certain preset values of the field.

In contrast to the optimal conditions for diffraction measurements with a pulsed magnetic field on a pulsed neutron source, where the duration of the source burst is near the duration of the magnetic pulse, it is advisable in the case of measurements with inelastic coherent scattering in inverse geometry (with monochromatization of scattered neutrons) to have a burst duration which is considerably less than the duration of the magnetic field pulse in order to get good field and energy resolutions. This condition is especially easy to satisfy on the ISIS spallation source where, for instance at a neutron wavelength of *3.5 Å*, the half-height neutron peak spread is *70 μs* [40].

Of course, measurements of inelastic scattering using a pulsed magnetic field are possible only on neutron sources with the highest peak thermal neutron fluxes. The measurement duration that is necessary for determining the phonon or magnon peak position on SNIM-2-IBR-2 (in inverse geometry) and on the spectrometers of ISIS is from *0.25* to *20 hours* for samples with a volume of several cm^3, depending on the geometry of scattering and the value of the neutron energy change. The duration of measurements with a magnetic field will be increased in correspondence with the decrease in pulse frequency, relative to the neutron source frequency. The frequency of pulses with an amplitude from *120* to *200 kOe* and a duration of *1000 μs*, on SNIM-2, is about *5/2* sec^{-1}. However, for inelastic scattering measurements, it is necessary to increase the operating volume for the sample by several times in comparison with diffraction measurements and to increase the duration of the pulses by several times.

For an approximate estimate, it is possible to say that the heat emission in the magnet per pulse for inelastic scattering investigations in a *120 - 200 kOe* field will be *5-10 times* more than for diffraction measurements. Correspondingly, the duration of the measurements will be increased approximately *10 times* in comparison with measurements without the field. Therefore, at present, one may apparently hope for measurements not of full dispersion curves but only of limited sections of these curves.

There is a possibility to increase the measuring efficiency by using several monochromators with corresponding detectors in the secondary beams, keeping condition (9) satisfied for each of them, as on the PRISMA spectrometer. Since the measured magnon peaks along all scattered beam directions have to be in the region of the magnetic pulse, the total angular range of scattering can not be too large.

7. Kinetics of phase transitions and small angle scattering of neutrons

As it was remarked above, investigations of the kinetics of first order phase transitions are made at the SNIM-2 facility of the IBR-2 reactor. The obtained hysteresis patterns do not have a solid explanation yet, but at any rate, it is possible to believe that they are connected, first of all, with a time delay in the movement of the domain walls. In the future, the SNIM-2 facility will be complemented by a source of rectangular magnetic field

pulses of amplitudes up to *30 - 50 kOe*, durations up *300 μs* and front durations of *2 μs*. The critical fields for some phase transitions, for example at the spin-flop transition, are equal to *40 - 80 kOe*. In such cases, superimposing two pulses [69] would simpler: a half-sine wave pulse with an amplitude which does not quite reach the critical value and a second pulse on top of it with a relatively small amplitude but with good rectangular form. The use of rectangular magnetic field pulses and improvement of the time resolution up to *1-2 μs* will permit a better understanding of these hysteresis phenomena to be achieved. Then, we can proceed to the research of relaxation processes at phase reconstruction, which are directly connected with magnon-phonon and magnon-magnon interactions.

The technique of rectangular pulses may also be used in neutron diffraction research of phase decay processes. When a magnetic field exceeds the critical value, corresponding to the metastability limit at a first order transition, i.e., to the spinodaly point, the phase state becomes absolutely unstable and it disintegrates by means of the spontaneous appearance and growth of new phase domains. It is possible to try to observe dynamic-type magnetic solitons in this process of disintegration. By this we mean spatially localized excitations in magnetically ordered substances which can originate at first order magnetic phase transitions [70,71]. As an example, radial distributions of "magnetic densities" for spherical solitonic excitations in an antiferromagnetic substance under a magnetic field directed along the anisotropy axis, are presented in Fig.9. In this case, Q corresponds to the value of the antiferromagnetism vector component which is normal to the anisotropy axis, ρ corresponds to the radius (both in reduced units). The magnitudes $n = 1, 2, 3$ designate solitons of the first three orders.

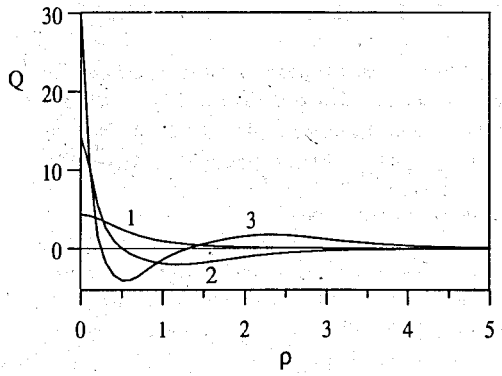

Fig.9 Radial distribution of the "magnetic density" in a spherical soliton originating at a first order phase transition.

Spherical solitons of analogous configurations can originate at other first order reorientation phase transitions. It follows from theory that when the field value corresponds to the metastability range, the formation of solitons has a threshold character, i.e., at each value of the field, the soliton energy can have values starting from a definite value. The energy of such excitations decreases near the spinodaly points. At disintegration of the phase state, the soliton energy becomes negative relative to the initial state, i.e., solitons can arise spontaneously. The radius of such solitons is on the order of *100 Å*. Magnetic solitons are virtually the ordered germs of a new phase state. Whereas, at a field value less

than the spinodaly point, the emerging solitons collapse, it is possible to expect that above the spinodaly point they can become the macroscopic domains of a new phase state.

The dynamic type magnetic solitons are exotic objects in the physics of condensed matter, and have not been observed in experiments, yet. It is possible that the phase transition represents an unique situation in which they can be manifested. But, this is not a simple task in an experiment. The preset value of the field should be reached quickly so that phase reconstruction by means of the growth of domains originating at different inhomogeneities (impurity inclusions, crystallite boundaries, domain boundaries of the initial state) will not materialize before the metastability state is reached. The specific character of the solitons, as different from other germs of the new phase, consists in the fact that they have a definite configuration (amplitude and form), are described by the motion equations, have a relatively small size and, possibly, a comparatively long lifetime. Therefore, it is possible to try to extract the neutron diffraction on solitons from diffraction scattering on the bulk of a crystal.

First of all, if the mosaicity of the crystal is small enough, the entire intensity of the diffraction peak in the process of phase reconstruction should be appreciably increased due to the small size of the solitons originating in large quantity at the phase disintegration. Besides, the soliton configuration should be manifested in a definite angle distribution of the neutron diffraction near the Bragg direction. In the last case, the standard technique of small angle scattering near the Bragg position of the crystal is applicable. The only complications are connected with the necessity of quick changes in the field value and with the time analysis of the neutron scattering.

8. Conclusion

At present, there is experience in using pulsed magnetic fields in neutron investigations at the pulsed reactors IBR (*6 kW* in the rare burst regime), IBR-30 and IBR-2 and at the spallation source KEK. In addition, several diffraction measurements with a pulsed field at a steady state reactor are known. Not only the pulsed neutron sources are suitable for such research. Steady-state reactors with a high flux of thermal neutrons are appropriate for diffraction investigations on single crystals with a pulsed magnetic field on the order of 10^5 *Oe*. Single pulsed thermal reactors in the single burst regime are also suitable for diffraction measurements. The instantaneous flux of thermal neutrons at the IBR-2 reactor, at the spallation source of ISIS and at designed spallation sources with power of about *5 MW* is sufficient for some experiments using inelastic coherent scattering on single crystals with a pulsed magnetic field of such value. The IBR-2 reactor is especially suitable due to its low cycle frequency. The peak flux of certain single pulse neutron sources permits the possibility of diffraction experiments with ultra-strong magnetic fields (> 10^6 Oe).

In our opinion, the use of a pulsed magnetic field in combination with neutron scattering may be prospective for the following research:

1) Determination of quasi-stationary magnetic structures induced by an external field.

2) Studying reorientation kinetics and relaxation processes at first order magnetic phase transitions.

3) Investigation of magnetic interactions by means of measuring dispersion relations at the action of an external field using inelastic coherent neutron scattering.

4) The quest for "exotic" magnetic excitations - quasi-particles in crystals, such as spatially localized dynamic type solitons, which probably originate at the first order transition. For that, it is possible to use diffraction measurements at the phase disintegration, including small angle diffraction scattering near the Bragg positions of the crystal.

Considerations expressed in this work are applicable not only to the use of pulsed magnetic fields in neutron investigations, but they are also true for other cases of condensed matter research at abrupt changes of an external action, for example, at pulsed pressures or pulsed electric fields.

Thanks are due to K.Krezhov and Yu.N.Pokotilovskii for very useful discussions of the perspectives of using pulsed magnetic fields in combination with pulsed neutron sources and to Ann Schaeffer for help in preparing the paper for publication.

References

1. V.V.Nietz, JINR, 3-5372, Dubna, 1970.
2. Kim Chil Sung and V.V.Nietz, phys. stat. sol., (a) 89 (1985) 45.
3. P.S.Antzupov, R.A.Voskanyan, R.Z.Levitin, V.V.Nietz, S.Niziol, R.P.Ozerov, Pak Gvan O and S.Shafran, JINR, P14-4548, Dubna, 1969; Solid State Physics (USSR), 13 (1971) 56.
4. R.Z.Levitin, V.V.Nietz, S.Niziol and R.P.Ozerov, Solid State Comm. 7 (1969) 1665.
5. V.V.Nietz, Solid State Comm., 30 (1979) 71.
6. V.V.Nietz, JINR, P13-10071, Dubna, 1976.
7. V.V.Nietz, G.Repke, Z.Tucharz and A.A.Yakovlev, JINR, P3-10072, Dubna, 1976.
8. A.V.Androsov et al., JINR, 13-11559, Dubna, 1978.
9. T.Giebultovitch, V.V.Nietz, A.A.Yakovlev and E.Yarotzki, JINR, P14-11558, Dubna, 1978.
10. V.V.Nietz and G.Repke, Solid State Physics (USSR) 23 No.1 (1981) 64.
11. T.Giebultovitch, V.V.Nietz, Z.Tucharz, A.A.Yakovlev and E.Yarotzki, Solid State Physics (USSR) 23 No.1 (1981) 233.
12. B.N.Ananiev et al., JINR, P13-89-517, Dubna, 1989.
13. G.A.Varenik et al., JINR, P13-89-518, Dubna, 1989..
14. D.Georgiev, V.V.Nietz and A.A.Yakovlev, JINR, P14-92-399, Dubna, 1992.
15. D.Georgiev, V.V.Nietz, A.P.Sirotin and A.A.Yakovlev, JINR, P14-92-400, Dubna, 1992.
16. D.Georgiev, V.V.Nietz and A.P.Sirotin, JINR, P14-92-401, Dubna, 1992.
17. D.Georgiev, V.V.Nietz, T.B.Petukhova, A.P.Sirotin, G.A.Varenik and A.A.Yakovlev, to be published in Journal of Neutron Research, (1996).
18. D.Georgiev, V.V.Nietz, A.I.Ostrovnoy, T.B.Petukhova and A.P.Sirotin, JINR, P10-94-434, Dubna, 1994.
19. D.Georgiev and V.V.Nietz, JINR, P14-94-429, Dubna, 1994; J. of Magn. and Magn. Mater., 124 No1 (1996) 119.

20. S.A.Buyko, D.Georgiev, K.Krezhov, V.V.Nietz and G.Pasazhov, JINR, P14-94-431, Dubna, 1994; J. Phys. Cond. Matter, v.7 (1995) 8099.
21. Directory of Nuclear Reactors, Vienna, IAEA, vol.2, 1959; vol.5, 1964; vol.6, 1966; vol.8, 1970.
22. J.MacPhee and R.F.Lumb, in: Pulsed Neutron Reactors, vol.2, Vienna, IAEA, 1965, p.575.
23. Selected bibliography on pulsed reactors, J. Brit. Nucl. Energy Soc. 5 No.2 (1966) 136.
24. A.H.Spano, Nucl. Sci. Engng. 19 (1964) 172.
25. M.E.Remley, J.W.Flora, D.L.Hetrick et al, in: Peaceful Uses of Atomic Energy, vol.11, Geneva, 1958, P/1079, p.447.
26. A.I.Smirnov, V.M.Talizin and V.E.Chvostionov, Preprint of KIAE, IAE-1200, Moscow, 1966.
27. G.A.Freund, in: Peaceful Uses of Atomic Energy, vol.10, Geneva, 1958, P/1848, p.461.
28. I.V.Kurtchatov, S.M.Feinberg, N.A.Dollezhal et al, Atomnaya Energiya (USSR), 17 No.7 (1964) 463.
29. Yu.B.Khariton, A.M.Voinov, V.F.Kolesov at al, Voprosi sovremennoy experimentalnoy i teoreticheskoy physiki (USSR), Leningrad, Nauka, 1984, p.103-119.
30. R.Grossinger, G.Badurek, Ch.Gigler and Ch.Schotzko, Physica, Condensed Matter, B155 (1989) 392.
31. G.Badurek, Ch.Gigler, R.Grossinger and R.Kremenka, Report on Workshop on Pulsed Magnetic Field and Pulsed Neutron Sources, Abingdon, Oxfordshire, UK, 29-30 June, 1995.
32. A.Yamagishi and M.Date, in the Proceedings of the 1982 International Symposium on High Field Magnetism, ed. M.Date, North-Holland, Amsterdam, p.289, 1983.
33. A.Yamagishi and M.Date, Physica, B155 (1989) 91.
34. M.Motokawa, H.Nojiri, J.Ishihara and K.Ohnishi, Physica B155 (1989) 39.
35. H.Nojiri, M.Uchi, S.Watamura, M.Motokawa, H.Kawai, Y.Endoh and T.Shigeoka, Journ. Phys. Soc. Japan 60 No.7 (1991) 2380.
36. N.Nojiri, M.Motokawa, N.Nishida and Y.Endoh, Intern. Conf. on Neutr. Scattering, Oxford, UK, August, 1991, S1-A-4.
37. M.Motokawa, H.Nojiri, M.Uchi, S.Watamura, H.Kawai and Y.Endoh, Proceedings of The 11th Meeting of International Collaboration on Advanced Neutron Sources (KEK, Tsukuba, October, 1990), vol.2 (1991) p.979.
38. M.Motokawa, H.Nojiri and Y.Endoh, Physica B177 (1992) 279.
39. M.Motokawa, M.Arai, M.Mino, K.Ubukata, T.Bokui and M.Fujita, Proceedings of The 12th Meeting of International Collaboration on Advanced Neutron Sources (Abingdon, Oxfordshire, UK, May, 1993), vol.1 (1994) p.I-260.
40. U.Steigenberger, Workshop on Pulsed Magnetic Field and Pulsed Sources, Abingdon, Oxfordshire, UK, 29-30 June, 1995.
41. C.J.Carlile, M.A.Adams, J.B.Forsyth, P.S.R.Krishna, Proceedings of the Twelfth Meeting of the International Collaboration on Advanced Neutron Sources, ICANS-XII, 24-28 May, 1993, Abingdon, Oxfordshire, UK, vol.1, p.I-73.

42. H.Lengerer, Proceedings of the Twelfth Meeting of the International Collaboration on Advanced Neutron Sources, ICANS-XII, 24-28 May, 1993, Abingdon, Oxfordshire, UK, vol.2, p.P-1.
43. C.M.Fowler, W.B.Garn and R.S.Caird, J.Appl.Phys., 31 (1960) 588.
44. A.D.Sakharov, R.Z.Lyudaev, E.N.Smirnov, Yu.I.Plyushchev, A.I.Pavlovskiy et al., Dokladi Akademii Nauk SSSR (USSR), 196 No.1(1965) 65.
45. A.D.Sakharov, Uspekhi Fizitcheskikh Nauk (USSR), 88 No.4 (1966) 725.
46. H.Knopfel and F.Herlach, eds., Proc. Conf. Megagauss Magnetic Field Generation by Explosives and Related Experiments, Frascati, 21-23 Sept. 1965 (Euratom, Brussels, 1966).
47. E.C.Cnare, J. Appl. Phys. 37 (1966) 3812.
48. C.M.Fowler, R.S.Caird, J.H.Fritz et al., Tech. Rep., LA-5065 (1972).
49. H.Knopfel, Pulsed High Magnetic Field (North-Holland, Amsterdam-London), 1970.
50. F.Herlach and H.Knopfel, Rev. Sci. Instrum., 36 (1965) 1088.
51. P.J.Turchi ed., Proc. 2nd Int. Conf. on Megagauss Magnetic Field Generation and Related Topics, Washington, D.C. 30 May - 1 June 1979 (Plenum, New York, 1980).
52. V.M.Titov and G.A.Shvetsov, eds., Proc. 3rd Int. Conf. on Megagauss Magnetic Field Generation and Related Topics, Novosibirsk, 13-17 June 1983 (Nauka, Moscow, 1984).
53. C.M.Fowler, R.S.Caird and D.J.Erickson, eds., Proc. 4th Int. Conf. on Megagauss Magnetic Field Generation and Related Topics, Santa Fe, 14-17 July (Plenum, New York, 1986).
54. A.I.Pavlovskii, N.P.Kolokolchikov, M.I.Dolotenko et al., Pis'ma v ZhETF (USSR) 27 (1978) 283.
55. A.I.Pavlovskii, N.P.Kolokolchikov, M.I.Dolotenko et al., PTE (USSR) 5 (1979) 195.
56. A.I.Pavlovskii and R.Z.Lyudaev, in: Problems of Modern Experimental and Theoretical Physics, A.P.Alexandrov, ed. (Leningrad, Nauka, 1984), p.206.
57. A.I.Pavlovskii, M.I.Dolotenko, N.P.Kolokolchikov, Pis'ma JETP (USSR), 38 No.9 (1983) p.437.
58. A.I.Pavlovskii, Priroda (USSR), No.8, August 1990, p.39.
59. N.Miura, T.Goto, K.Nakao, S.Takeyama, T.Sakakibara, T.Haruyama and T.Kikuchi, Physica B155 (1989) 23.
60. D.F.Wood, P.D.O'Brien and T.F.Wimett, in: Fast Burst Reactors. Proc. of National Topical Meeting on Fast Burst Reactors held at the University of New Mexico, Albuquerque, January 28-30, 1969. USAEC CONF-690102, 1969, p.81.
61. R.M.Jefferson, in: Fast Burst Reactors. Proc. of National Topical Meeting on Fast Burst Reactors held at the University of New Mexico, Albuquerque, January 28-30, 1969. USAEC CONF-690102, 1969.
62. R.L.Coats and P.D.O'Brien, Trans. of Americ. Phys. Nuclear Society 11 (1968) 219.
63. L.M.Choate and T.R.Schmidt, IEEE Transactions on Nuclear Science, vol.NS-25, No.6 (1978) 1625.
64. A.Bombik, V.V.Nietz and A.A.Yakovlev, JINR, P13-10070, Dubna, 1976.
65. S.Niziol, V.V.Nietz, R.P.Ozerov and A.A.Yakovlev, Solid State Physics (USSR), 15 No.7 (1973) 2151.
66. Guide to neutron research facilities at the ILL, Grenoble, France, 1994, p.9.

67. E.Malishevski, T.A.Matchekhina, V.V.Nietz and Pak Gvan O, JINR, P14-4270, Dubna, 1969.
68. Annual Report of ISIS, 1990 (RAL, Chilton, UK) p.26.
69. D.Georgiev, V.V.Nietz, V.A.Savin and A.A.Yakovlev, JINR, P13-89-579, Dubna, 1989.
70. V.Yu.Bezzabotnov, V.V.Nietz and S.A.Oleynik, JINR, P17-95-87, Dubna, 1995.
71. V.V.Nietz and S.A.Oleynik, JINR, P17-95-88, Dubna, 1995.

Received by Publishing Department
on May 27, 1996.